

RSC Advances



This is an *Accepted Manuscript*, which has been through the Royal Society of Chemistry peer review process and has been accepted for publication.

Accepted Manuscripts are published online shortly after acceptance, before technical editing, formatting and proof reading. Using this free service, authors can make their results available to the community, in citable form, before we publish the edited article. This *Accepted Manuscript* will be replaced by the edited, formatted and paginated article as soon as this is available.

You can find more information about *Accepted Manuscripts* in the [Information for Authors](#).

Please note that technical editing may introduce minor changes to the text and/or graphics, which may alter content. The journal's standard [Terms & Conditions](#) and the [Ethical guidelines](#) still apply. In no event shall the Royal Society of Chemistry be held responsible for any errors or omissions in this *Accepted Manuscript* or any consequences arising from the use of any information it contains.

COMMUNICATION

Natural biological template for ZnO nanoparticle growth and photocatalytic dye degradation under visible light

Cite this: DOI: 10.1039/x0xx00000x

Received 00th January 2012,
Accepted 00th January 2012Mengxiao Sun,^{ab‡} Tianhang Li,^{c‡} Zhaoyuan Zhang,^{d‡} Nana Wang,^a Aming Xie,^{*a}
Xuliang Lv,^{*b} Yuan Wang,^a Fan Wu,^{*a} Mingyang Wang^a

DOI: 10.1039/x0xx00000x

www.rsc.org/

Luffa sponge was used as a biotemplate for the growth of ZnO nanoparticles. This new structure of ZnO displayed a unique photocatalytic performance for dyes degradation under visible light.

Serious environment problems have aroused due to the increasing amount of wastewater generated by the industries. Wastewater generally contained organic dyes which were toxic and not suitable for being treated directly with a biological method, thus a novel technique which was efficient, inexpensive and “green” was required to chemically transfer them to non-hazardous compounds.¹ Various methods have been developed to remove dyes from water, such as physical or chemical adsorption,^{2,3} chemical oxidation,⁴ electrochemical oxidation⁵ and photodegradation.^{1,6-15} As a renewable energy source, sunlight is the most attractive power source for catalytic degradation and H₂ production,¹⁶⁻¹⁸ it delivers about 3×10²¹ kJ of energy to the earth surface per year. In the past few decades, the photocatalytic degradation of organic dyes employing the wide bandgap semiconductors under UV irradiation has been proven to be a very effective process.^{6,9,11,13} However, the wide bandgap semiconductors, such as TiO₂ and ZnO, can only absorb light with wavelengths below 380 nm to generate electron-hole pairs, which initiates photo degradation.¹ Unfortunately, UV light in solar irradiation is less than 5% and is too low to achieve significant photodegradation over a short time. As is known to us all, visible light (λ = 400-700 nm) accounts for ~50% of solar energy. Thus, it is more desirable to use visible light as the energy source for the degradation of the organic dyes. Accordingly, many efforts have been devoted to the development of photocatalysts which work under visible light. In this work, ZnO nanoparticles were grown on luffa sponge and used as photocatalysts for degradation of dye under visible light. Furthermore, the as-prepared ZnO structures exhibited

sufficient visible light degradation performance against methylene blue (MB) and rhodamin B (RhB).

Experimental section

Materials. Natural luffa sponge was purchased from Shi Wang (Shanghai) International INC., China. All reagents were of analytical grade and used without further purification. Distilled water was obtained from Direct-Q3 UV, Millipore.

Synthesis of biotemplate based ZnO structure. Natural luffa sponge was cut into small cube and heated in a tubular furnace at 600 °C for 4 hours in vacuum. Then, the resulted carbonized luffa sponge was immersed in a solution of HNO₃ for 24 hours and carboxyl groups formed on its surface. After washing with water, the sponge was soaked into a solution of Zn(NO₃)₂ (0.5 M) and aged for 4 hours. As a result, Zn²⁺ ions were attached on the surface of the sponge. At last, the sponge was annealed in a tubular furnace at 600 °C for 4 hours under atmosphere, and the biotemplate based ZnO structure was obtained.

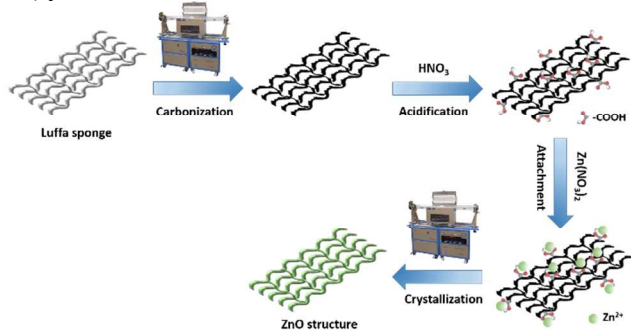
Characterization. The morphology of the as-prepared sample was characterized with a field emission scanning electron microscope (FE-SEM, S-4800, Hitachi) and a field emission high resolution transmission electron microscope (FE-HRTEM, Tecnai G2 F20 UTwin, FEI). Energy dispersive X-ray (EDX) analysis was also carried out with a transmission electron microscope (TEM, Tecnai G2 F30 STwin, FEI). Powder diffraction data of the as-synthesized sample was collected from 10° to 80° in 2θ using an X-ray diffractometer (XRD, D/MAX TTRIII, Rigaku) with Cu Kα (λ = 1.5418 Å) radiation. Raman spectroscopy was carried out on a Renishaw in Via

Raman Microscope equipped with 532 nm laser. Brunauer-Emmett-Teller (BET) specific surface area was carried out on a 3H-2000BET-A instrument (Beishide Instrument-ST Co., Ltd.)

Dye photocatalytic activity test. The photodegradation of MB and RhB dyes was observed on the basis of the absorption spectroscopic technique. In a typical process, photocatalysts were mixed with an aqueous solution of dye (2×10^{-5} M, 100 mL) in a vessel. And then the vessel was exposed to the UV-light curing system with 250 W high pressure Hg lamp (UV-1318, Zhuhai Kaivo Optoelectronic Technology Co., Ltd., China) or the solar simulator equipped with a 150 W xenon lamp (SS150, Zolix Instruments CO., Ltd., China) under continuous stirring. Then, the solution was analyzed by recording the UV-vis spectrum of dyes at the maximum absorbance.

Results and discussion

The synthesis process and the digital photo have been showed in Scheme 1 and Fig. 1, respectively. In brief, natural luffa sponge was cut into small cubes, followed by carbonization and acidization process to form biotemplates. Natural luffa sponge consisted of irregular fibers (Fig. 2a), these structures were maintained even after carbonization (Fig. 2b, c and d). Zn^{2+} would be attached on the surface of the template due to its electronegativity,¹⁹ and the following heat treatment turned them to ZnO. Fig. 3a and b showed FE-TEM images of the as-prepared ZnO structure. The irregular fiber-like structures were retained in the final products and the ZnO structure was composed of nanoparticles which attached on the surface of fibers. The peaks of C, O and Zn elements are presented in EDX spectra (Fig. 3c), confirming the existence of ZnO and carbonized fibers. Moreover, the peaks of Si, S and Ca should be the impurities which were the components of natural luffa sponge. HRTEM images displayed in Fig. 3d and e show that the lattice spacing is 0.28 nm, which corresponds to the d-spacing of (010) and (100) planes of ZnO.



Scheme 1 Synthesis strategy of biotemplate based ZnO structure.



Fig. 1 Digital photo of luffa sponge, carbonized product and as-prepared ZnO structure.

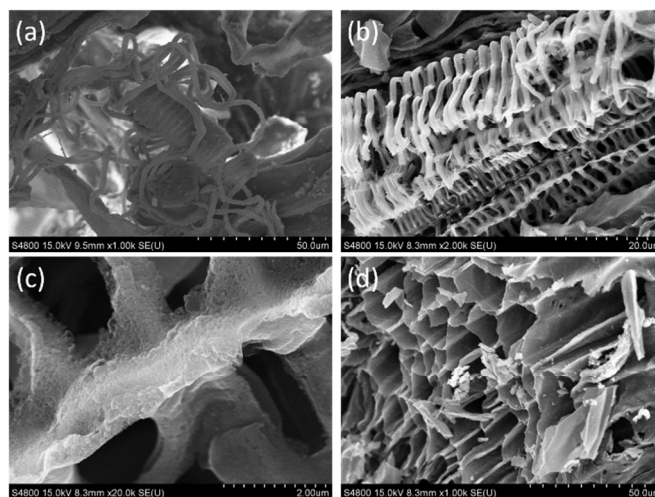


Fig. 2 SEM images of luffa sponge before (a) and after (b, c and d) carbonization.

X-ray powder diffraction pattern of the as-prepared ZnO structure was given in Figure 4a. All the sharp diffraction peaks at 31.8° , 34.5° , 36.3° , 47.6° , 56.6° , 63.0° , 68.1° and 69.2° can attributed to reflections 100, 002, 101, 102, 110, 103, 112 and 201 of hexagonal ZnO according to ICDD PDF No. 79-0206. Furthermore, the peak at 23.3° corresponds to the (002) plane of graphite²⁰ and the peak at 29.5° is due to an unidentified impurity.

In a perfect ZnO crystal, first-order Raman scattering are caused by the optical phonons at Γ point of Brillouin zone. Group theory predicts the existence of the following optic modes:

$$\Gamma_{\text{opt}} = A_1 + 2B_1 + E_1 + 2E_2 \quad (1)$$

Both A_1 and E_1 modes are polar and split into transverse optical (TO) and longitudinal optical (LO) components. E_2 mode consists of two modes of low and high frequency phonons, which is associated with the vibration of the heavy Zn sublattice and oxygen atoms, respectively. B_1 branch is silent in ZnO structure,²¹ each active vibration mode corresponds to a band in the Raman spectrum and the intensity of them depends on scattering cross section of these modes.

In Fig. 4b, E_2 (high) mode at 438 cm^{-1} dominate in the nonresonant Raman scattering spectra, indicating that the sample has perfect crystal quality. The obvious peak at 380 cm^{-1} is attributed to A_1 (TO) mode. The optical phonon overtone with A_1 symmetry locate at 331 cm^{-1} . The peak at 1087 cm^{-1} and the broad band at 1153 cm^{-1} are the acoustic combination of A_1 and E_2 .¹⁸ Peaks at 582 , 713 and 995 cm^{-1} should belong to the muliphonons process.²²

The BET specific surface area of as-prepared ZnO structure is $179 \text{ m}^2 \text{ g}^{-1}$, which is much higher than the commercial ZnO ($35 \text{ m}^2 \text{ g}^{-1}$). We believe that the increase in surface area is benefit from the hollow structure of biotemplate and it will enhance the photodegradation performance of ZnO.

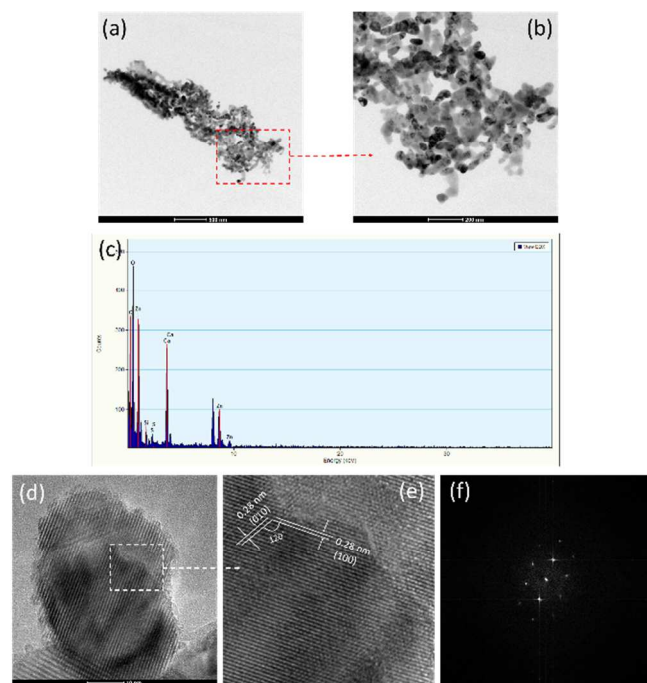


Fig. 3 FE-TEM images (a, b), EDX spectrum (c), HRTEM images (d, e) and selected area electron diffraction (SAED) pattern of the as-prepared ZnO structure (f).

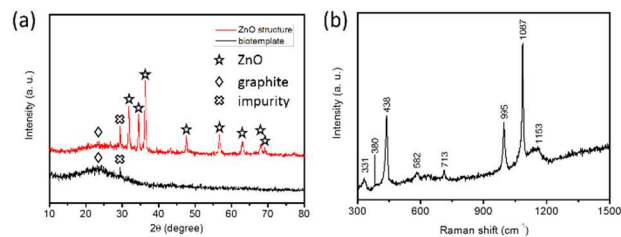


Fig. 4 (a) XRD patterns of the carbonized luffa sponge (black) and as-prepared ZnO structure (red); (b) Raman spectrum of the as-prepared ZnO structure.

The potential application of the ZnO structure as an organic pollutant scavenger was investigated by MB and RhB model probes. As shown in Fig. 5a to c, the UV absorption intensity of solutions with various concentrations of ZnO decreased rapidly in 15 min. Fig. 5d showed the time dependent normalized concentrations of MB solution under simulated UV irradiation in the presence of different concentration of ZnO structure. The Y -axis was reported as C/C_0 , where C_0 and C were the initial and actual concentration of dye solution at different reaction times, respectively. With ZnO structure in solution (0.5 mg mL^{-1}), the degradation of MB could be completed within 30 min.

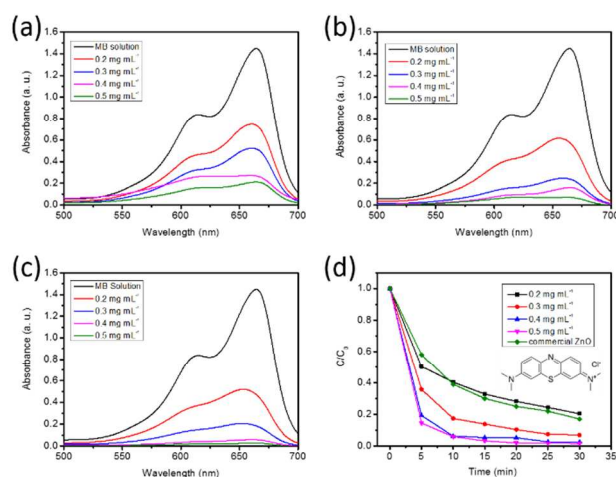


Fig. 5 UV-vis absorption spectra of MB solution which was degraded by the as-prepared ZnO structure after 5 min (a), 10 min (b) and 15 min (c) under UV light; The time-dependent normalized concentration of MB solutions in the presence of ZnO structure of various concentration, the concentration of commercial ZnO is 0.5 mg mL^{-1} (d).

Under visible light irradiation, the absorption intensity of MB and RhB solutions also decreased when ZnO structure was introduced (Fig. 6a to c and Fig. 7a), indicating that the photocatalytic reaction destroyed the chromophoric structure of the dye. As shown in Fig. 6d, with an addition of a low concentration (0.5 mg mL^{-1}) of ZnO to the MB solution, dye degraded completely within 120 min under irradiation. Fig. 6e showed the visual effects of MB degradation process. Furthermore, 80% of RhB can be degraded by 0.5 mg mL^{-1} of ZnO within 320 min under the visible light irradiation (Fig. 7b).

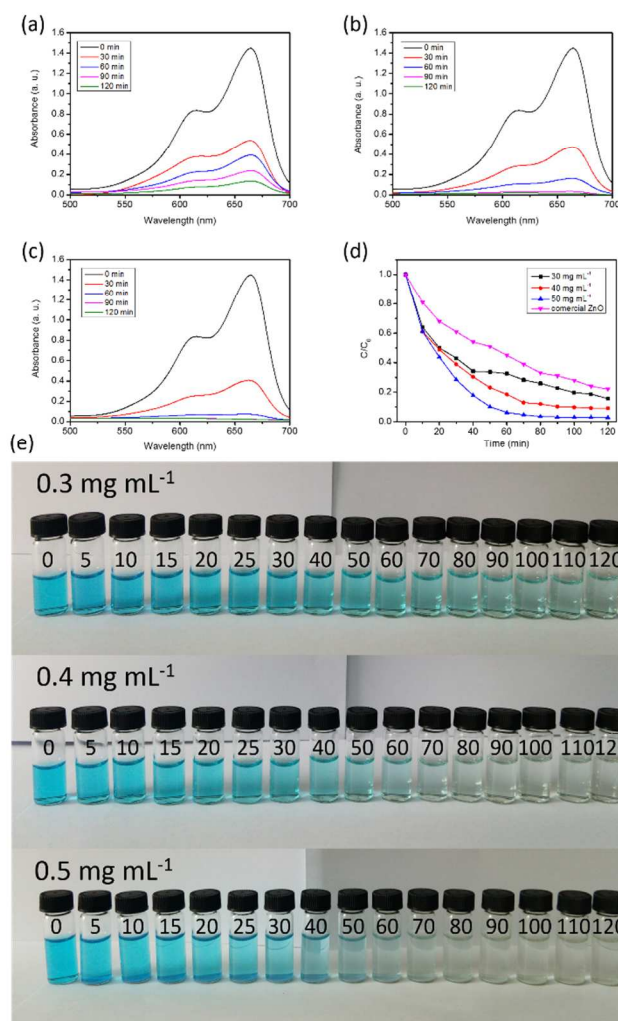


Fig. 6 UV-vis absorption spectra of MB solution which was degraded by the as-prepared ZnO structure with the concentration of 0.3 (a), 0.4 (b) and 0.5 (c) mg mL^{-1} under standard sunlight; photodegradation of MB with different concentration of as-prepared ZnO structure, the concentration of commercial ZnO is 0.5 mg mL^{-1} (d); digital photos of degraded MB solutions with the elapsed time labelled on each flask (e).

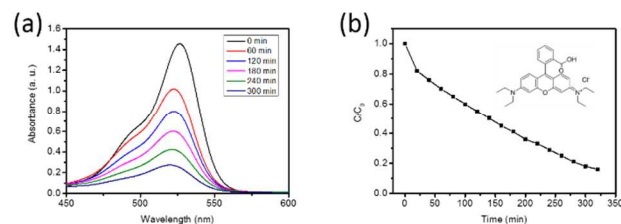


Fig. 7 UV-vis absorption spectrum of RhB solution which was degraded by as-prepared ZnO structure with the concentration of 0.5 mg mL^{-1} (a) under standard sunlight and photodegradation of RhB with as-prepared ZnO structure (b).

Conclusions

In summary, ZnO nanoparticles were successfully grown on the surface of luffa sponge. The obtained ZnO structure was demonstrated to be of highly photocatalytic activity to the degradation of dyes in the industrial wastewater under UV and

visible light irradiation. It can be expected that our findings will provide new material for environmental protection.

Acknowledgements

This work was financially supported by the National Natural Science Foundation of China (51403236) and the Opening Project of State Key Laboratory of Disaster Prevention & Mitigation of Explosion & Impact (DPMEIKF201310).

Notes and references

^a State Key Laboratory for Disaster Prevention & Mitigation of Explosion & Impact, PLA University of Science and Technology, Nanjing 210007, P. R. China. wufanjlg@163.com (F. Wu) aminghugang@126.com (A. Xie)

^b Key Laboratory of Science and Technology on Electromagnetic Environmental Effects and Electro-optical Engineering, PLA University of Science and Technology, Nanjing 210007, P. R. China. xllu1957@126.com (X. Lv)

^c Anqing No. 2 Middle School, Anqing 246003, P. R. China.

^d Nanjing Foreign Language School, Nanjing 210018, P. R. China.

Electronic Supplementary Information (ESI) available: [details of any supplementary information available should be included here]. See DOI: 10.1039/c000000x/

- J. Zhao, K. Wu, T. Wu, H. Hidaka and N. Serpone, *J. Chem. Soc., Faraday Trans.*, 1998, **94**, 673.
- H. Bi, X. Xie, K. Yin, Y. Zhou, S. Wan, L. He, F. Xu, F. Banhart, L. Sun and R. S. Ruoff, *Adv. Funct. Mater.*, 2012, **22**, 4421.
- C. Namasivayam and D. Kavitha, *Dyes Pigm.*, 2002, **54**, 47.
- C. Flox, S. Ammar, C. Arias, E. Brillas, A. V. Vargas-Zavala and R. Abdelhedi, *Appl. Catal. B*, 2006, **67**, 93.
- G. Ciardelli and N. Ranieri, *Water Res.*, 2001, **35**, 567.
- L. Kuang, Y. Zhao and L. Liu, *J. Environ. Monit.*, 2011, **13**, 2496.
- F. Ruggieri, A. A. D'Archivio, M. Fanelli and S. Santucci, *RSC Adv.*, 2011, **1**, 611-618.
- K. Zhou, Y. Zhu, X. Yang, X. Jiang and C. Li, *New J. Chem.*, 2011, **35**, 353.
- T. Kou, C. Jin, C. Zhang, J. Sun and Z. Zhang, *RSC Adv.*, 2012, **2**, 12636.
- J. Sun, Y. Yuan, L. Qiu, X. Jiang, A. Xie, Y. Shen and J. Zhu, *Dalton Trans.*, 2012, **41**, 6756.
- S. Singh, K. C. Barick and D. Bahadur, *J. Mater. Chem. A*, 2013, **1**, 3325.
- X. Yin, H. Zhang, P. Xu, J. Han, J. Li and M. He, *RSC Adv.*, 2013, **3**, 18474.
- Z. Zhang, F. Xiao, Y. Guo, S. Wang and Y. Liu, *ACS Appl. Mater. Interfaces*, 2013, **5**, 2227.
- C. Mondal, J. Pal, M. Ganguly, A. K. Sinha, J. Jana and T. Pal, *New J. Chem.*, 2014, **38**, 2999.
- X. Liu, W. Li, N. Chen, X. Xing, C. Dong and Y. Wang, *RSC Adv.*, 2015, **5**, 34456.
- C. Wang, J. Li, X. Lv, Y. Zhang and G. Guo, *Energ. Environ. Sci.*, 2014, **7**, 2831.
- J. Ran, J. Zhang, J. Yu and S. Qiao, *ChemSusChem*, 2014, **7**, 3426.
- J. Ran, J. Zhang, J. Yu, M. Jaroniec and S. Qiao, 2014, **43**, 7787.

Journal Name

- 19 D. V. Kosynkin, A. L. Higginbotham, A. Sinitskii, J. R. Lomeda, A. Dimiev, B. K. Price and J. M. Tour, *Nature*, 2009, **458**, 872.
- 20 F. Wu, Y. Xia, Y. Wang and M. Wang, *J. Mater. Chem. A*, 2014, **2**, 20307.
- 21 R. Zhang, P. Yin, N. Wang and L. Guo, *Solid State Sci.*, 2009, **11**, 865.
- 22 J. M. Calleja and M. Cardona, *Phys. Rev. B*, 1977, **16**, 3753.